Cell Proliferation

Cell Prolif., 2013, **46**, 695–704 doi: 10.1111/cpr.12073

BMP4 promotes vascularization of human adipose stromal cells and endothelial cells *in vitro* and *in vivo*

C. Zhou*, X. Cai*, B. E. Grottkau† and Y. Lin*,†

**State Key Laboratory of Oral Diseases, West China Hospital of Stomatology, Sichuan University, Chengdu, 610041, China and †Department of Orthopaedic Surgery, MassGeneral Hospital for Children and the Pediatric Orthopaedic Laboratory for Tissue Engineering and Regenerative Medicine, Harvard Medical School, Boston, MA, 02114, USA*

Received 10 May 2013; revision accepted 11 August 2013

Abstract

Objectives: Vascularization is a major obstacle to clinical application of regenerative medicine. Engineered tissues must be able to generate an early vascular network that can quickly connect with the host vasculature. Recent research demonstrates that natural adipose tissues contain abundant stromal cells, which can give rise to pericytes. In this study, we aimed to investigate the application of human adipose stromal cells (ASCs) to vascularization, and the function of BMP4 protein during vascularization.

Materials and methods: Immunofluorescence staining for α-SMA and PDGFR-β were utilized to identify characteristics of ASCs/pericytes. They were then loaded into a collagen-fibronectin gel with endothelial cells to assess their vascularization ability, both *in vitro* and *in vivo*.

Results: We showed that the ASCs expressed some of the essential markers of pericytes and they were able to promote vascularization with endothelial cells in 3D culture, both *in vitro* and *in vivo*. BMP4 protein further promoted this vascularization.

Conclusion: Adipose stromal cells promoted vascularization by endothelial cells and BMP4 protein further enhanced this effect.

Correspondence: B. E. Grottkau, Department of Orthopaedic Surgery, MassGeneral Hospital for Children and Pediatric Orthopaedic Laboratory for Tissue Engineering and Regenerative Medicine, Harvard Medical School 15 Parkman St Boston, MA 02114, USA. Tel.: (617) 726-8523; Fax: (617)724-0551; E-mail: bgrottkau@partners.org/Y. Lin, State Key Laboratory of Oral Diseases, West China Hospital of Stomatology, Sichuan University, #14 3rd section of south Renmin Road, Chengdu 610041, China. E-mail: yunfenglin@scu.edu.cn

Introduction

Tissue engineering and regenerative medicine have progressed rapidly in recent years (1); their goal being to reconstruct and restore function of damaged or diseased tissues (2). Two necessary conditions for success include appropriate cells for seeding plus a biodegradable scaffold, to produce an artificial environment that mimics *in vivo* conditions (3). At present, vascularization is one of the most formidable clinical obstacles to application of tissue-engineered constructs. The central portion of a construct is remote from obtaining sufficient nutrition in the early stages of a procedure, which results in necrosis, inflammation and ultimate failure of the implant (4). Engineered tissues must have be able to generate early vascular networks that can quickly anastomose with the host circulatory system (5).

Simplistically, blood vessels consist of endothelial cells and surrounding supporting cells, the latter ultimately forming the external wall of the blood vessel (6). Several studies have demonstrated that formation of robust and functional engineered vascular networks requires co-implantation of endothelial cells and mesenchymal stem cells (7–9). Human adipose tissue stem cells (ASCs) have proven ability to be induced to differentiate into chondrocytes, adipocytes, osteoblasts, endothelial cells or myocytes. Adipose tissue is derived from the embryonic mesenchyme and has a stromal structure, similar to that of bone marrow stem cells (BMSCs) (8,10). Compared to BMSCs, ASCs are much more abundant and easier to obtain, involving relatively lower donor site morbidity. There is almost no cell heterogeneity between ASCs, but obvious heterogeneity between BMSCs, resulting from the mixture of haematopoietic and mesenchymal stem cells. It is believed ASCs represent an ideal substitute for BMSCs to be used in tissue engineering and regenerative medicine (11).

BMP4 is necessary for mesodermal formation and vascular/haematopoietic specification in several species (12); effects of BMP4 on development have been well documented in many. Recent work has demonstrated that BMP4 enhances formation and outgrowth of the immature vascular system (13,14). During embryonic development, up-regulation of BMP4 leads to increase in numbers of blood vessels, whereas inhibition of BMP4 by noggin results in reduction in number of blood vessels (15,16). In the field of tissue engineering, most previous work with BMP4 has been in bone and cartilage formation; there are few reports regarding the role of BMP4 in vascularization (17).

In this study, we have attempted to use human adipose tissue stem cells (hASCs) and human umbilicus vein endothelial cells (HUVECs) to form vascular networks *in vitro* and *in vivo*. We then studied function of BMP4 protein in the process of vascularization.

Material and methods

Isolation and culture of human adipose stromal cells

hASCs were obtained from clinically discarded human adipose tissues with IRB approval. First, the adipose tissues were washed extensively in saline and then were digested in 0.075% type I collagenase (Sigma-Aldrich, St. Louis, MO, USA) for 45 min at 37 °C. Cells released were filtered and collected by centrifugation at 1200 ***g*** for 5 min. Cell pellets were then washed 3 times in culture medium and seeded into flasks, in control medium containing α-MEM, 10% foetal bovine serum (FBS), 100 units/ml penicillin, and 100 μg/ml streptomycin. The cells were maintained in a humidified atmosphere of 5% CO_2 at 37 °C and were used at passage 2 for the following experiments.

Morphological evaluation and labelling of hASCs

The hASCs were labelled with eGFP by lentivirus vector. Immunofluorescence staining for α-SMA and PDGF-Rβ was carried out to distinguish the type of hASCs. α-SMA and PDGF-Rβ are markers of pericytes; if the hASCs expressed both α-SMA and PDGF-Rβ, it would indicate that they shared lineage derivation with pericytes.

For immunostaining, cells were blocked in 1% bovine serum albumin and 0.1% Triton at room temperature for 30 min. Specimens were then incubated for 1 h at 4 °C with mouse anti-human monoclonal antibodies against α-SMA (Dako, Glostrup, Denmark) and PDGF-Rβ (Sigma, St. Louis, MO, USA). They were then incubated in secondary goat anti-mouse IgG Alexa Fluor 594 (Invitrogen, Eugene, OR, USA) for 30 min.

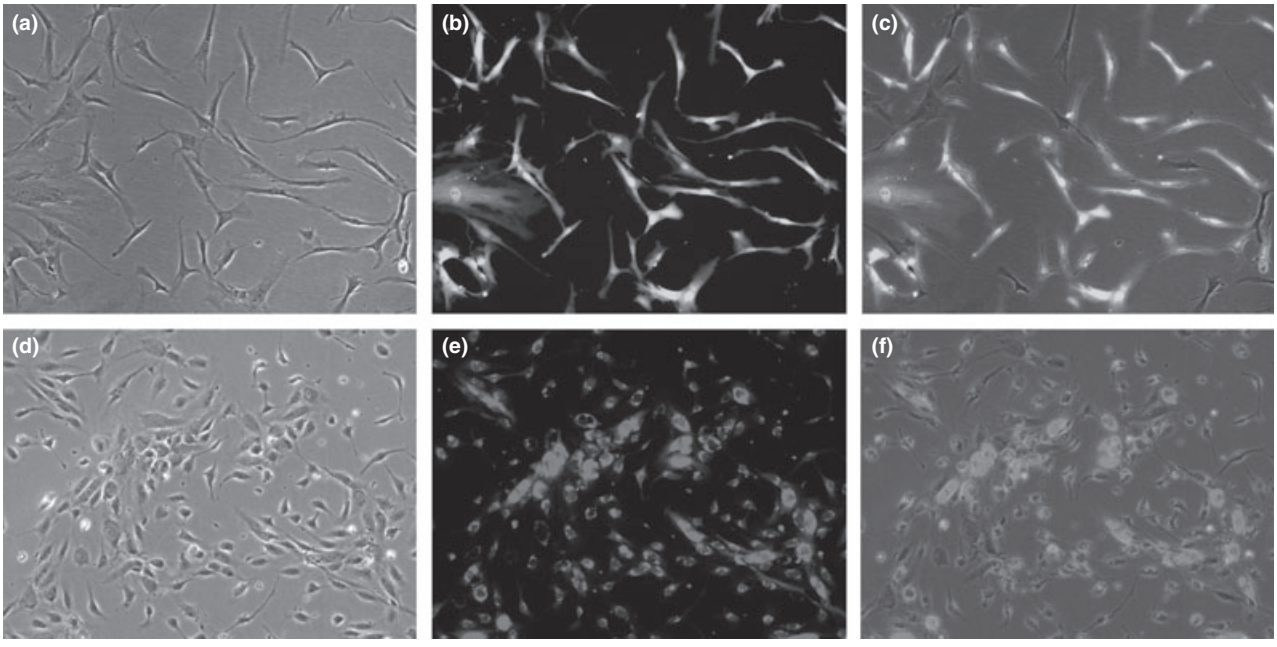

Figure 1. Human adipose stromal cells are fibroblast-like and GFP-positive (a–c). Human umbilical vein endothelial cells (HUVECs) demonstrated red fluorescence positivity (d–f) (×200).

Human umbilical vein endothelial cell preparation and labelling

HUVECs were labelled with DsRed by lentivirus vector. They were then maintained in 0.1% gelatin-coated plates in endothelial cell growth medium (EGM-2; Lonza, Hopkinton, MA, USA).

3D collagen/fibronectin gel preparation and formation of vascular network in vitro

Collagen/fibronectin gels were prepared as previously described with minor modification. HUVECs and hASCs were mixed 4:1 ratio and suspended in gel (ml), which included 1.5 mg/ml collagen gel PureCol® EZ Gel (Advanced BioMatrix, San Diego, CA, USA), 90 μg/ml human plasma fibronectin (Gibco, Bedford, MA, USA), 25 mM HEPES (Gibco, Grand Island, NY, USA), 38.5% complete EGM-2 (Lonza), with final cell concentration 2×10^6 cells/ml. Experimental group A was HUVECs and hASCs, group B was group A with addition of 2 ng/ml BMP4 protein, group C was group A with 10 ng/ml BMP4 protein. The control group had HUVECs alone. Cell suspensions were polymerized in a 48-well plate (100 μl/well) for 30 min at 37 °C and gels were then covered with 250 μl complete EGM-2 medium. To quantify formation of vascular networks, an overview of the whole gel was observed under a DMi 6000-B microscope (Leica, Wetzlar, Germany), then three representative fields were selected in each group. One image was captured for each field and average area of vascular network was analysed by ImagePro (Media Cybernetics, Rockville, MD, USA), as described in our previous studies (18,19).

Formation of vascular networks in vivo

Two month old female nude mice were anesthetized with 0.4 mg/g avertin. In experimental group 1, 250 μl

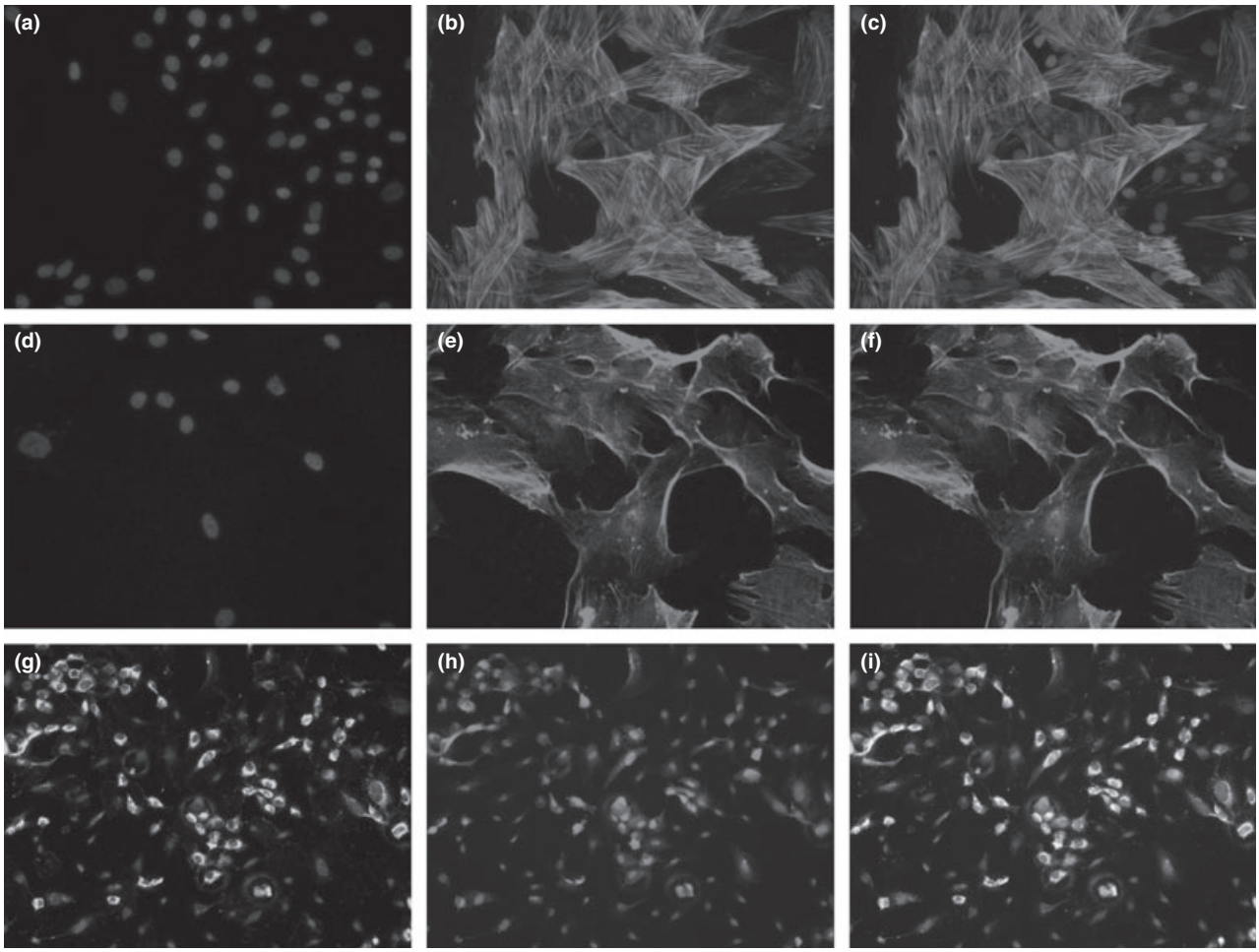

Figure 2. hASCs were α-SMA-positive (a–c) and PDGF-Rβ-positive (d–f) with red fluorescence. HUVECs were vWF-positive (g) as shown by green fluorescence. HUVECs were labelled with dsRED lentivirus (i). Merged picture shows overlay of green staining and red labelling (h).

mixture of collagen/fibronectin gel was loaded with HUVECs and hASCs. Experimental group 2 consisted of the 250 μl mixture of collagen/fibronectin gel loaded with HUVECs and hASCs plus 10 ng/ml BMP4 protein. In the control group, 250 μl mixture of collagen/fibronectin gel was loaded with HUVECs only; the blank group represented an injection of pure collagen/fibronectin gel without cells. Gels were injected subcutaneously to the dorsum of each mouse. At 1 week and 2 weeks after implantation, mice were euthanized (n = 3 for each

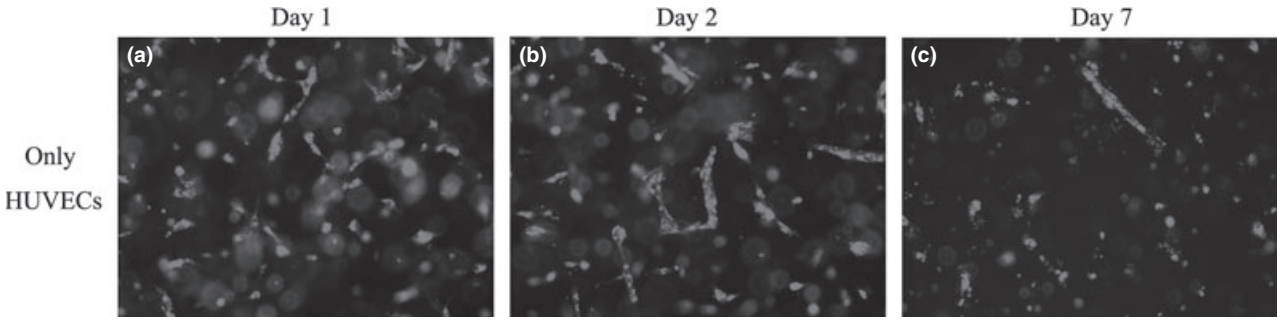

Figure 3. In the control group, HUVEC cultures without hASCs proliferated slowly and did not form vascular networks at days 1, 2 or day 7 (a–c).

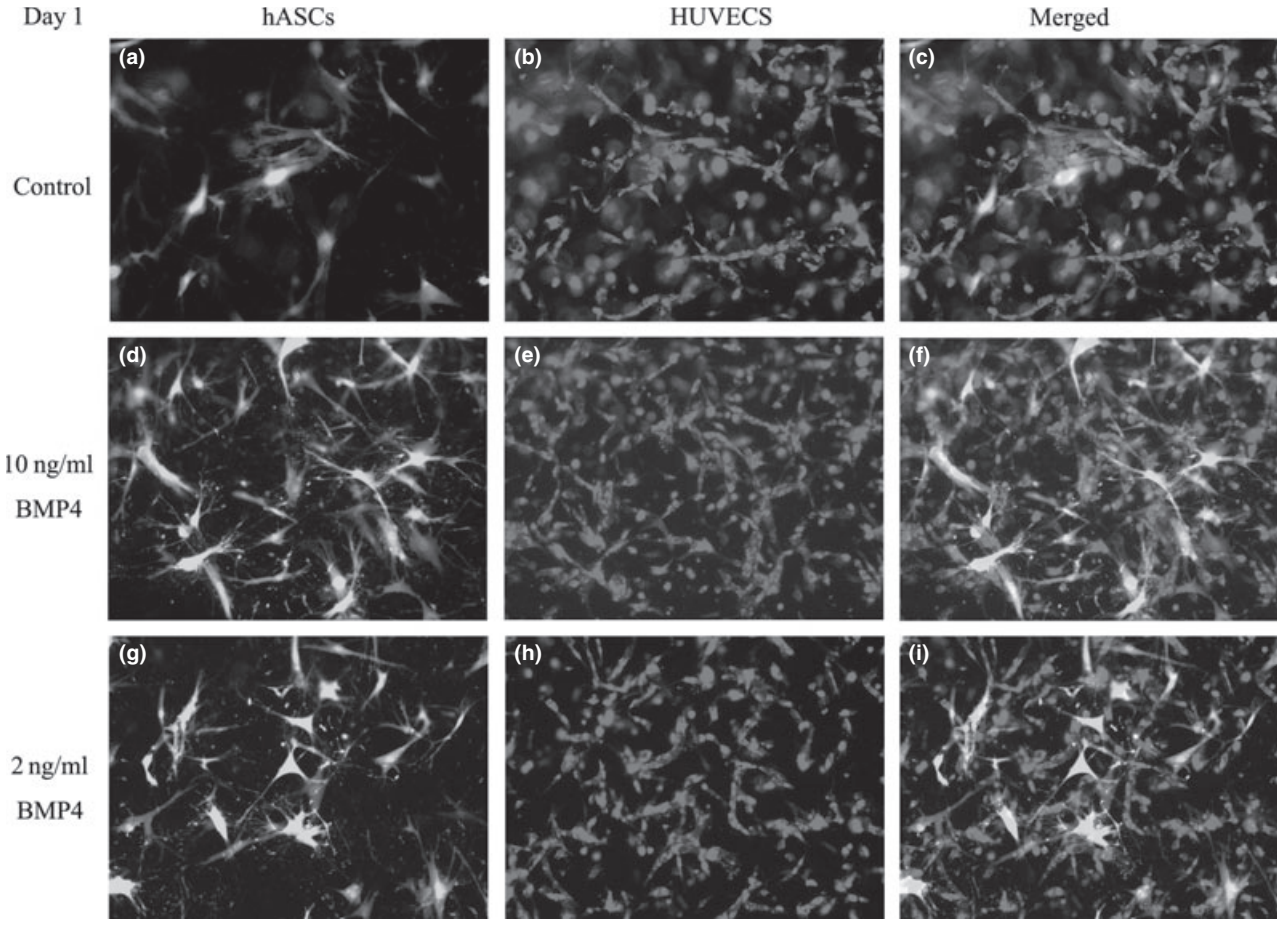

Figure 4. Formation of 3D vascular network *in vitro* by day 1. In experimental group A, ASCs are labeled with GFP (a). HUVECs were cultured with hASCs. HUVECs began to proliferate and contact each other to form short tubule-like structures (a, b). hASCs were found distributed around the HUVECs (c). In group B, more tubule-like structures were observed (d–f). Group C was similar to group B (g–i).

time point). Implanted constructs were then carefully separated from surrounding fibrous capsules, washed in PBS and immediately observed under a laser scanning confocal microscope (Nikon A1, Kyoto, Japan). Three representative fields were selected in each group and one image was captured for each field. All images were analysed by ImagePro software to evaluate formation of new blood vessels, as described in our previous studies (18,19).

Data analysis

Each experiment was repeated a minimum of three times and representative data are presented as means ± SD. ANOVA was used to analyse differences within groups in all assays above. To specify significant differences between experimental groups and controls, Dunnett *t*-testing was conducted. $P < 0.05$ indicates significant differences in all *t*-tests.

Results

Morphological and immunolabel identification of hASCs and HUVECs

The labelled human adipose stromal cells were polygonal in shape and GFP-positive (Fig. 1a–c). The labelled human umbilical vein endothelial cells had cobblestone appearance and were red fluorescence-positive (Fig. 1d–f).

α-SMA and PDGF-Rβ immunostaining of hASCs indicated that most of them were α-SMA (Fig. 2a–c) and PDGF-Rβ-positive (Fig. 2d–f). vWF staining of HUVECs was positive (Fig. 2g–i).

Formation of vascular networks within 3D collagen/fibronectin gels in vitro

The ability of hASCs to assist HUVECs in forming and maintaining a vascular network was evaluated by

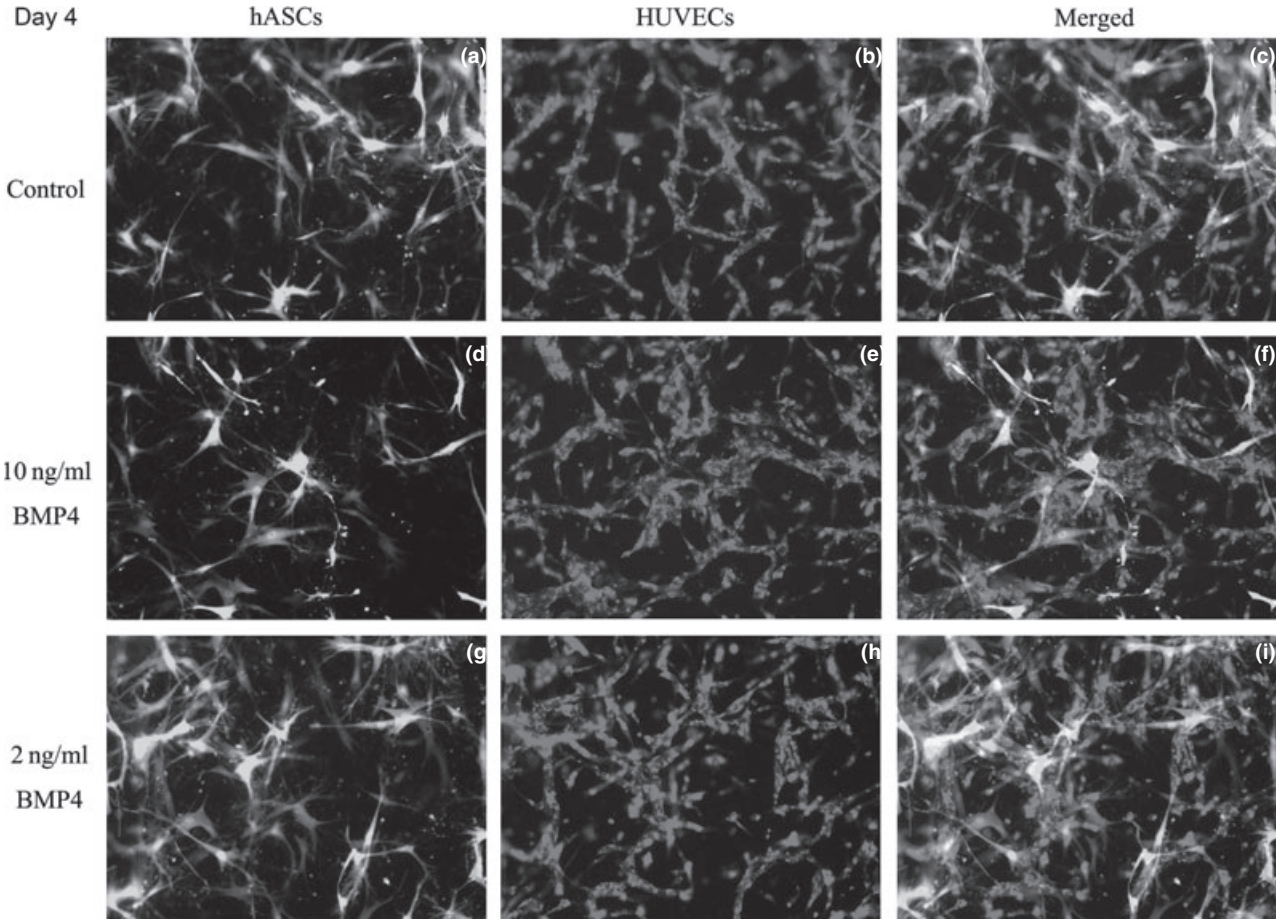

Figure 5. Formation of 3D vascular networks *in vitro* by day 2. At day 4, more ASCs labeled with GFP can be found on the gel (a). HUVECs formed tube-like structures that connected to one another (a, b), while hASCs were distributed around the tubules (c). In group B, tubule-like structures were more complex and more dense than those of group A (d–f). In group C, numbers of tubule like structures fell between groups A and B (g–i).

loading them into 3D collagen-fibronectin gels *in vitro*. Gels were cultured and observed using fluorescence microscopy; they demonstrated the presence of an extensive vascular network.

In the control group, HUVECs cultured without hASCs proliferated slowly and did not form vascular networks by days 1, 2, or day 7 (Fig. 3a–d).

At day 1 in experimental group A, in which HUVECs were cultured with hASCs, the HUVECs began to proliferate and form contacts with other cells; also they created some short tubule-like structures (Fig. 4a). hASCs were distributed around the HUVECs (Fig. 4b, c). In group B, more tubule-like structures were observed (Fig. 4d–f); group C was similar to group B (Fig. 4g–i).

By day 4, the HUVECs formed tube-like structures and connected to each other (Fig. 5a), while the hASCs were distributed around the tubules (Fig. 5b,c). In group B, tubule-like structures were more complex and more dense than those of group A (Fig. 5d–f). In group C, the tubule-like structures were denser than in groups A and B (Fig. 5g–i).

By day 7, networks were primarily formed by HUVECs (Fig. 6a) and hASCs grew denser around the networks (Fig. 6b,c). Networks of group B were more complex and denser than group A networks (Fig. 6d–f), while in group C, density of networks was higher compared to either group A or group B (Fig. 6g–i).

Formation of vascular structures was analysed by software in each group at varying time points. The control group (HUVECs only) at day 1 was set to be the standard. At day 1 in experimental group A (HUVECs + hASCs), formation of vascular structures increased by a factor of 2.394 ± 0.089, group B (HUVECs + ASCs + 2 ng/ml BMP4 protein) increased by 2.791 ± 0.870 and group C (HUVECs + ASCs+10 ng/ml BMP4 protein) increased by 3.199 ± 0.591. This represented a significant increase for each experimental group compared to controls ($P < 0.05$), but there was

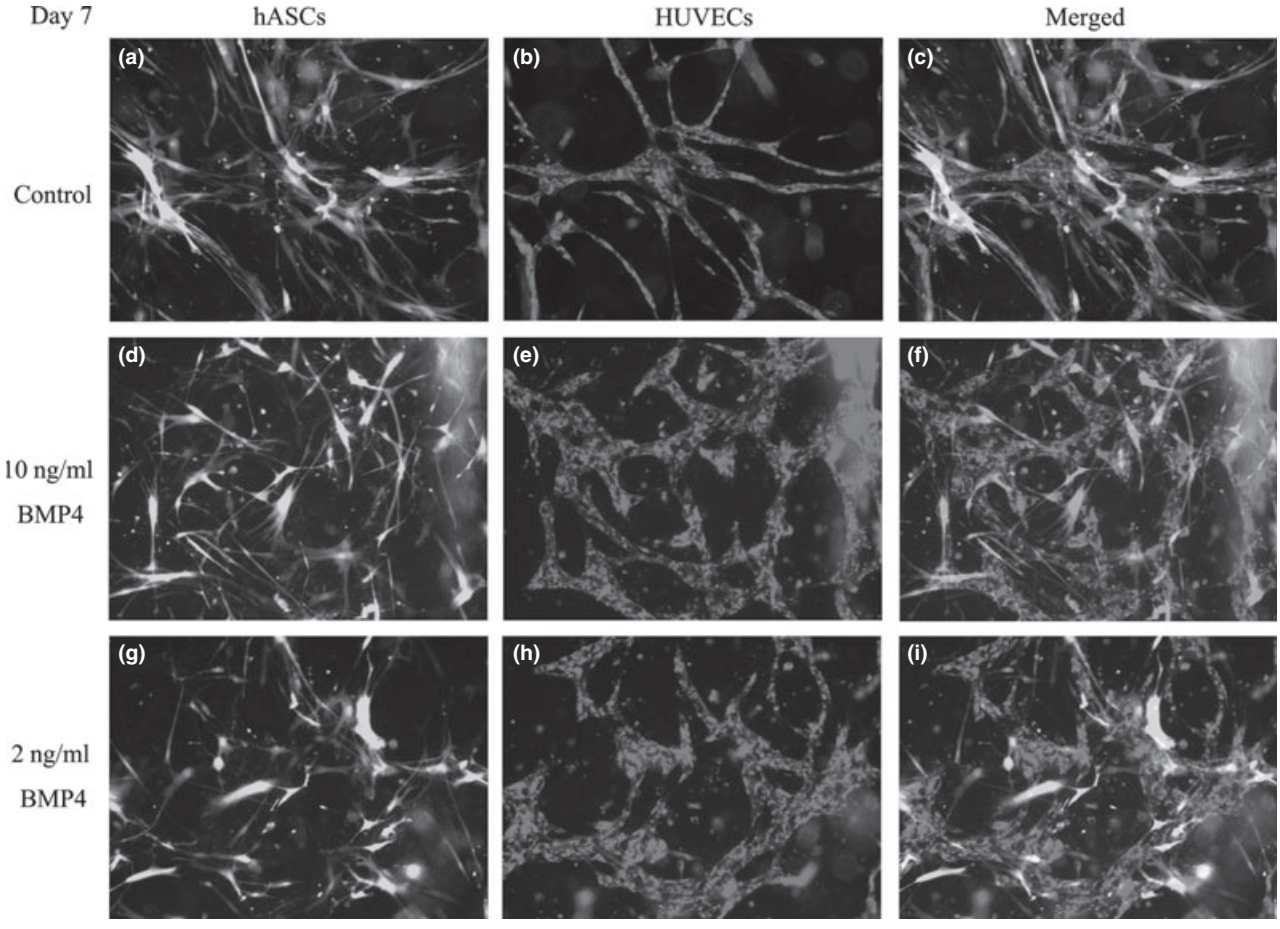

Figure 6. Formation of 3D vascular network *in vitro* by day 7. At day 7, ASCs proliferate with their GFP labeling (a). vascular networks were primarily formed by HUVECs (a, b), with hASCs coalesced around them (b, c). Group B network was more complex and more dense than that of group A (d–f). In group C, density of the network was higher than either group A or B (g–i).

no significant difference between experimental groups (Fig. 7). At day 4 in the control group (HUVECS alone), formation of vascular structures was 0.697 ± 0.082 compared to baseline, while group A (HUVECS + hASCs) increased 2.538 ± 0.421-fold, group B (HUVECs + ASCs + 2 ng/ml BMP4 protein) increased 3.760 ± 0.369-fold and group C (HUVECs + ASCs + 10 ng/ml BMP4 protein) increased 4.138 ± 0.757-fold. There were significant differences between experimental groups and the control group. Groups B and C were significantly higher than group A ($P < 0.05$) (Fig. 7). At day 7, formation of vascular structures in the control group (HUVECS alone) measured 0.429 ± 0.047, while experimental group A (HUVECs + hASCs) increased 2.267 ± 0.193-fold, group B (HUVECs + ASCs + 2 ng/ml BMP4 protein) increased 2.858 ± 0.634-fold, and group C (HUVECs + ASCs + 10 ng/ml BMP4 protein) increased 3.840 ± 1.301-fold over baseline. There were significant differences between the experimental groups and the control group. Group C was significantly higher than groups A and B ($P < 0.05$) (Fig. 7).

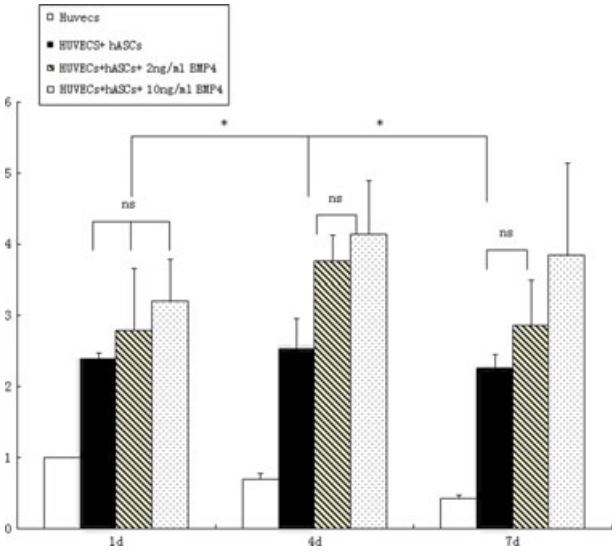

Figure 7. Formation of vascular structures was analysed by the appropriate software at different groups and time points. The control group (HUVECs only) at day 1 was set as being the standard. At day 1 (1 d), conditions in all experimental groups had significant differences from the control group ($P < 0.05$), but there were no significant differences between experimental groups. At day 4 (4 d), there were significant differences between experimental groups and control groups; experimental groups B and C were significantly higher than group A ($P < 0.05$). At day 7 (7 d), there were significant differences between experimental groups and the control group with group C being significantly higher than groups A and B ($P < 0.05$). Asterisk stands for $P < 0.05$; ns, non-significance.

Formation of vascular networks within 3D collagen/fibronectin gels in vivo

To evaluate blood vessel formation of hASCs, cells seeded in the collagen/fibronectin gels were subcutaneously implanted into nude mice. Size of *in vivo* implants became smaller over time reducing to around 20% of their original size, after 2 weeks.

In the control group (HUVECs alone), some discontinuous blood vessels formed by red HUVECs were observed by 1 week after implantation (Fig. 8a). These vessels became continuous and more complex by 2 weeks (Fig. 8d). In experimental group 1 (HUVECs + ASCs), continuous red vessel networks of red labelled HUVECs were observed at 1 week and 2 weeks. These networks were surrounded by green ACSs (Fig. 8b,e). At both week 1 and 2, more networks containing continuous red vessels were observed in experimental group 2 (HUVECs + ASCs + 10 ng/ml BMP4) than in group 1 and the control group. Red vessels were surrounded by green ASCs (Fig. 8c,f). Two weeks after implantation, many more robust networks were observed in group 1 than in the control group. Again, these networks were surrounded by abundant green ASCs (Fig. 8f). Blank control injections of pure collagen/fibronectin gel disappeared and nothing was retrieved after 1 week.

Formation of vascular structures was analysed by ImagePro in each group at specified intervals, the control group at 1 week being set as standard. Formation of vascular structures in experimental group 1 increased to 1.958 ± 0.450 times the control, while group 2 increased to 2.683 ± 0.524 over control values. Significant differences existed between experimental groups and the control group with group 2 being significantly higher than group A ($P < 0.05$) (Fig. 9).

By 2 weeks, formation of vascular structures in the control group increased to 1.266 ± 0.173, while formation of vascular structures in experimental group 1 increased to 2.058 ± 0.432, and in group 2 to 2.998 ± 0.379. Again, there were significant differences between experimental groups and the control group with group 2 significantly higher than group 1 ($P < 0.05$) (Fig. 9).

Discussion

Rapid vascularization is crucial for success of clinical application of tissue engineered constructs, as diffusion cannot provide sufficient oxygen and nutrients to cells in the centre of an implant (20,21). Lack of vascularization results in necrosis or inflammation and subsequent failure of the tissue implantation or transplantation (22).

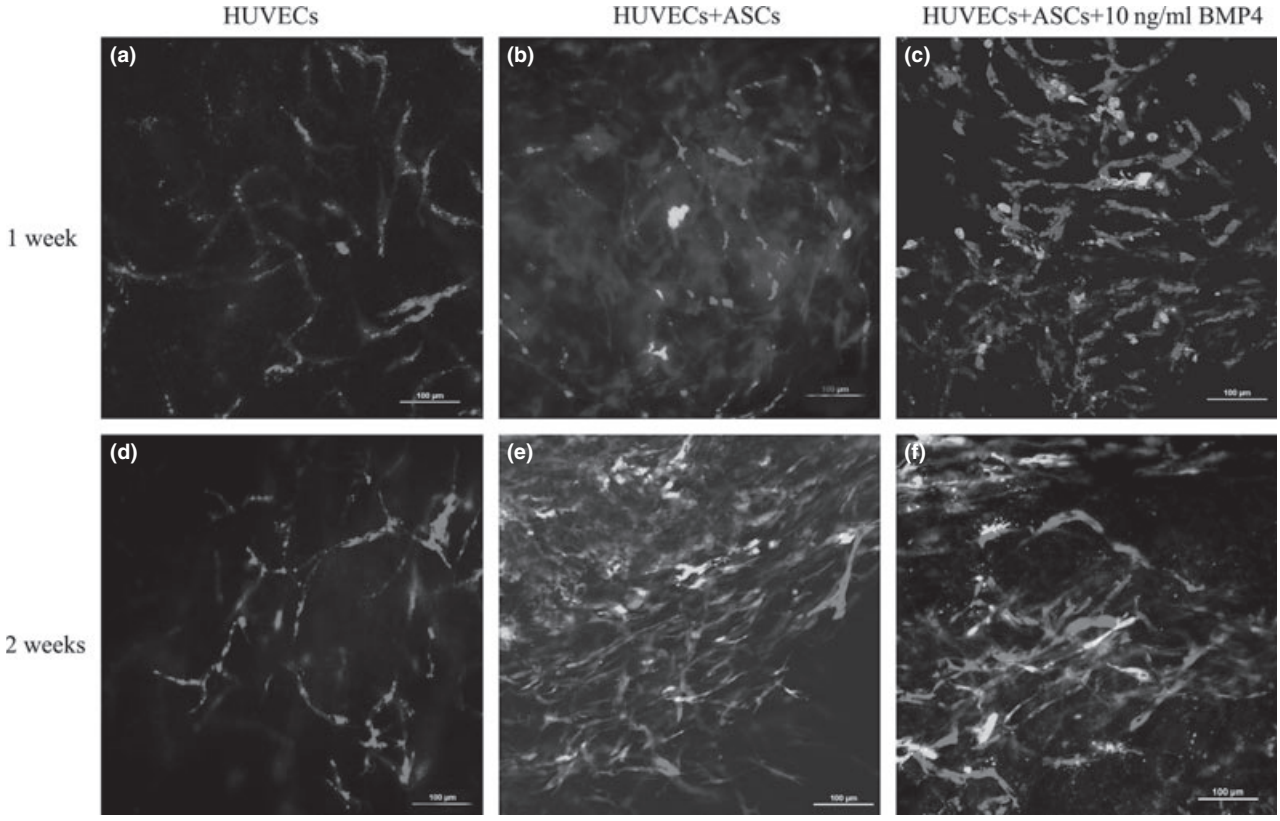

Figure 8. Formation of 3D vascular networks *in vivo*. In the control group (HUVECs only), some discontinuous blood vessels formed by red HUVECs were observed by 1 week after implantation (a). These vessels became continuous and more complex by 2 weeks (d). In experimental group 1 (HUVECs + ASCs), continuous red networks were observed at 1 week. This network was surrounded by green ASCs (b). Two weeks after implantation, many more robust networks were observed, and these were surrounded by an abundance of green ASCs (e). In experimental group 2 (HUVECs + ASCs + 10 ng/ml BMP4), many more continuous red networks were observed than in group 1 and the control group, at 1 week. This network was surrounded by green ASCs (c). Two weeks after implantation, more vascular networks were observed than in group 1 and the control group, and these networks were supported by an abundance of green ASCs (f).

In this study, we used ASCs as a supportive population for vascularized tissue engineering constructs, and BMP4 as accelerator, to initiate rapid vascularization of tissue engineering prostheses. Our data indicate that ASCs not only demonstrated multilineage differentiation ability but also had supportive effects on vascular formation by endothelial cells, which could be further enhanced by BMP4.

Vascularization is a process of blood vessel formation occurring by endothelial progenitor cell differentiation, migration and interconnection in response to stimulators (such as growth factors and cell-cell contact) to form new blood vessels (23). During vascularization, pericytes are recruited to surround the endothelial cells as supporting cells, to stimulate their proliferation and connection with each other (24). Then pericytes continue to assist endothelial cells in forming networks and to guide their maturation through direct contact mediated cell-cell interactions (25). Pericytes are also a type of smooth muscle cell - they express α-smooth muscle actin and form the external wall of blood vessels (26). Platelet-derived growth factor receptor (PDGFR)-β is a further marker that is commonly used to identify pericytes (27). Pericytes fulfil at least two important roles in assisting vascularization: (i) synthesis of growth factors and (ii) formation of the mural wall of new blood vessels. Control of both these mechanisms remain unclear at present (28), although a number of studies has proved that direct contact and communication between ECs and pericytes/smooth muscle cells are essential to vascularization (29).

The majority of ASCs used in this study expressed considerable amounts of the two important markers of pericytes. Even though we could not claim all these ASCs to be pericytes, it is not surprising that some of them could function as pericytes to support vascularization by endothelial cells. This is in agreement with our previous work, in which we showed that α-SMA-positive ASCs could promote vascularization by endothelial cells in 3D collagen gels (19). Supportive effects of

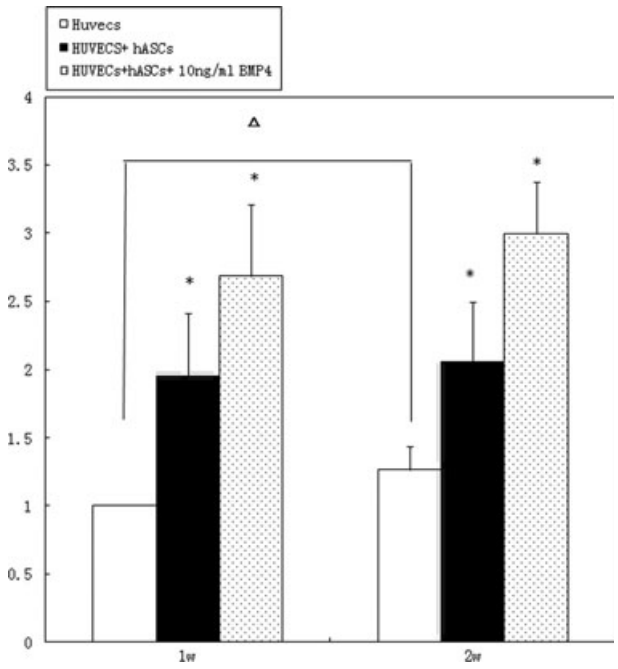

Figure 9. At 1 week (1 w), there were significant differences between conditions in experimental groups and the control group, with group B significantly higher than group A ($P < 0.05$). At 2 weeks (2 w), there were also significant differences between the experimental groups and control group, with group B being significantly higher than group A ($P < 0.05$). Asterisk stands for $P < 0.05$ comparing experimental groups with the control group at one time point; delta stands for $P < 0.05$ comparing the same group between different time points.

ASCs as pericytes were proposed to explain the important roles ASCs play in tissue repair (30). In avascular tissue, ASCs can increase matrix deposition of native cells by secreting growth factors (31). In highly vascular tissues, ASCs can initiate rapid vascularization by endothelial cells in injured sites by morphogen secretion or cell–cell contact (32). These two mechanisms could explain why ASCs promote tissue regeneration without differentiating into tissue-specific cells. In line with our data presented in this paper, similar results have been reported by others, showing that both BMSCs and ASCs help endothelial cells to organize into pre-vascular-like structures, with mechanisms involving cell–cell contacts and reciprocal signalling (33). In this study, we have provided more quantitative data on supportive effects of ASCs during vascularization.

A further point we would like to make here, is that viability of ASCs *in vivo* was very high even two weeks after implantation. It has been reported that allogenic transplantation of ASCs in rats has resulted in rapid cell replacement *in vivo*, indicated by quick disappearance of ASCs after implantation (34). In this study, we used nude mice as recipients for ASCs and achieved high levels of viability. As nude mice mainly have deficiency in the T cell-mediated immune response, our data suggest that the T cell-mediated immune response might play an important role in rapid turnover of tissue engineering constructs consisting of ASCs. However, more studies regarding immune responses to transplanted ASCs in recipients needs to be carried out to clarify this mechanism after transplantation.

Taken together in this study, we can once more confirm that co-culture or co-implantation of ASCs and HUVECs can benefit vascularization by endothelial cells. In addition to this, our data also indicate that beneficial effects of ASCs for vascularization can be further enhanced by stimulation with BMP4.

Acknowledgements

This work was funded by the Peabody Foundation, Inc., the Constance and Anthony A Franchi Fund for Pediatric Orthopaedics at the MassGeneral Hospital for Children, and National Natural Science Foundation of China (81071273, 31170929, 81201211), Foundation for the Author of National Excellent Doctoral Dissertation of China (FANEDD 200977), Doctoral Fund of Ministry of Education of China (20110181120071).

References

1 Langer R, Vacanti JP (1993) Tissue engineering. *Science* **260**, 920–926.
2 Caplan AI (2000) Tissue engineering designs for the future: new logics, old molecules. *Tissue Eng.* **6**, 1–8.
3 Cancedda R, Dozin B, Giannoni P, Quarto R (2003) Tissue engineering and cell therapy of cartilage and bone. *Matrix Biol.* **22**, 81–91.
4 Lovett M, Lee K, Edwards A, Kaplan DL (2009) Vascularization strategies for tissue engineering. *Tissue Eng. Part B. Rev.* **15**, 353–370.
5 Laschke MW, Strohe A, Scheuer C, Eglin D, Verrier S, Alini M *et al.* (2009) In vivo biocompatibility and vascularization of biodegradable porous polyurethane scaffolds for tissue engineering. *Acta Biomater.* **5**, 1991–2001.
6 Bagley RG, Weber W, Rouleau C, Teicher BA (2005) Pericytes and endothelial precursor cells: cellular interactions and contributions to malignancy. *Cancer Res.* **65**, 9741–9750.
7 Traktuev DO, Prater DN, Merfeld-Clauss S, Sanjeevaiah AR, Saadatzadeh MR, Murphy M *et al.* (2009) Robust functional vascular network formation in vivo by cooperation of adipose progenitor and endothelial cells. *Circ. Res.* **104**, 1410–1420.
8 Qi MC, Zou SJ, Han LC, Zhou HX, Hu J (2009) Expression of bone-related genes in bone marrow MSCs after cyclic mechanical strain: implications for distraction osteogenesis. *Int. J. Oral Sci.* **1**, 143–150.
9 Rangiani A, Cao ZG, Liu Y, Voisey Rodgers A, Jiang Y, Qin CL *et al.* (2012) Dentin matrix protein 1 and phosphate homeostasis

are critical for postnatal pulp, dentin and enamel formation. *Int. J. Oral Sci.* **4**, 189–195.
10 Lin Y, Chen X, Yan Z, Liu L, Tang W, Zheng X *et al.* (2006) Multilineage differentiation of adipose-derived stromal cells from GFP transgenic mice. *Mol. Cell. Biochem.* **285**, 69–78.
11 Lin YF, Jing W, Wu L, Li XY, Wu Y, Liu L *et al.* (2008) Identification of osteo-adipo progenitor cells in fat tissue. *Cell Prolif.* **41**, 803–812.
12 Towler DA (2009) Bone morphogenetic proteins. *Blood* **114**, 2012–2013.
13 Rothhammer T, Bataille F, Spruss T, Eissner G, Bosserhoff AK (2007) Functional implication of BMP4 expression on angiogenesis in malignant melanoma. *Oncogene* **26**, 4158–4170.
14 Heinke J, Wehofsits L, Zhou Q, Zoeller C, Baar KM, Helbing T *et al.* (2008) BMPER is an endothelial cell regulator and controls bone morphogenetic protein-4-dependent angiogenesis. *Circ. Res.* **103**, 804–812.
15 Boyd NL, Dhara SK, Rekaya R, Godbey EA, Hasneen K, Rao RR *et al.* (2007) BMP4 promotes formation of primitive vascular networks in human embryonic stem cell-derived embryoid bodies. *Exp. Biol. Med. (Maywood)* **232**, 833–843.
16 Zhou Q, Heinke J, Vargas A, Winnik S, Krauss T, Bode C *et al.* (2007) ERK signaling is a central regulator for BMP-4 dependent capillary sprouting. *Cardiovasc. Res.* **76**, 390–399.
17 Liu W, Oh SH, Kang Yk Y, Li G, Doan TM, Little M *et al.* (2003) Bone morphogenetic protein 4 (BMP4): a regulator of capsule chondrogenesis in the developing mouse inner ear. *Dev. Dyn.* **226**, 427–438.
18 Cai X, Lin Y, Friedrich CC, Neville C, Pomerantseva I, Sundback CA *et al.* (2009) Bone marrow derived pluripotent cells are pericytes which contribute to vascularization. *Stem Cell Rev.* **5**, 437–445.
19 Cai X, Lin Y, Hauschka PV, Grottkau BE (2011) Adipose stem cells originate from perivascular cells. *Biol. Cell* **103**, 435–447.
20 Rouwkema J, Rivron NC, van Blitterswijk CA (2008) Vascularization in tissue engineering. *Trends Biotechnol.* **26**, 434–441.
21 Kirkpatrick CJ, Unger RE, Krump-Konvalinkova V, Peters K, Schmidt H, Kamp G (2003) Experimental approaches to study vascularization in tissue engineering and biomaterial applications. *J. Mater. Sci. Mater. Med.* **14**, 677–681.
22 Schumann P, Tavassol F, Lindhorst D, Stuehmer C, Bormann KH, Kampmann A *et al.* (2009) Consequences of seeded cell type on vascularization of tissue engineering constructs in vivo. *Microvasc. Res.* **78**, 180–190.
23 Bryan BA, D'Amore PA (2008) Pericyte isolation and use in endothelial/pericyte coculture models. *Methods Enzymol.* **443**, 315–331.
24 Rajashekhar G, Traktuev DO, Roell WC, Johnstone BH, Merfeld-Clauss S, Van Natta B *et al.* (2008) IFATS collection: Adipose stromal cell differentiation is reduced by endothelial cell contact and paracrine communication: role of canonical Wnt signaling. *Stem Cells* **26**, 2674–2681.
25 Amos PJ, Shang H, Bailey AM, Taylor A, Katz AJ, Peirce SM (2008) IFATS collection: the role of human adipose-derived stromal cells in inflammatory microvascular remodeling and evidence of a perivascular phenotype. *Stem Cells* **26**, 2682–2690.
26 Armulik A, Abramsson A, Betsholtz C (2005) Endothelial/pericyte interactions. *Circ. Res.* **97**, 512–523.
27 Gerhardt H, Betsholtz C (2003) Endothelial-pericyte interactions in angiogenesis. *Cell Tissue Res.* **314**, 15–23.
28 Melero-Martin JM, De Obaldia ME, Kang SY, Khan ZA, Yuan L, Oettgen P *et al.* (2008) Engineering robust and functional vascular networks in vivo with human adult and cord blood-derived progenitor cells. *Circ. Res.* **103**, 194–202.
29 Loffredo F, Lee RT (2008) Therapeutic vasculogenesis: it takes two. *Circ. Res.* **103**, 128–130.
30 Caplan AI, Dennis JE (2006) Mesenchymal stem cells as trophic mediators. *J. Cell. Biochem.* **98**, 1076–1084.
31 Wu L, Prins HJ, Helder MN, van Blitterswijk CA, Karperien M (2012) Trophic effects of mesenchymal stem cells in chondrocyte co-cultures are independent of culture conditions and cell sources. *Tissue Eng. Part A* **18**, 1542–1551.
32 Huang W, Zhang D, Millard RW, Wang T, Zhao T, Fan GC *et al.* (2010) Gene manipulated peritoneal cell patch repairs infarcted myocardium. *J. Mol. Cell. Cardiol.* **48**, 702–712.
33 Verseijden F, Posthumus-van Sluijs SJ, Pavljasevic P, Hofer SO, van Osch GJ, Farrell E (2010) Adult human bone marrow- and adipose tissue-derived stromal cells support the formation of prevascular-like structures from endothelial cells in vitro. *Tissue Eng. Part A* **16**, 101–114.
34 Imanishi Y, Saito A, Komoda H, Kitagawa-Sakakida S, Miyagawa S, Kondoh H *et al.* (2008) Allogenic mesenchymal stem cell transplantation has a therapeutic effect in acute myocardial infarction in rats. *J. Mol. Cell. Cardiol.* **44**, 662–671.

